View metadata, citation and similar papers at core.ac.uk

brought to you by CORE

provided by Elsevier - Publisher Connector

The Influence of Lysolipids on the Spontaneous Curvature and Bending Elasticity of Phospholipid Membranes

N. Fuller and R. P. Rand

Department of Biological Sciences, Brock University, St.Catharines, Ontario L2S 3A1, Canada

ABSTRACT The effects of lysolipids on phospholipid layer curvature and bending elasticity were examined using x-ray diffraction and the osmotic stress method. Lysolipids with two different head groups, phosphatidylcholine (PC) and phosphatidylethanolamine (PE), and differing hydrocarbon chains were mixed with the hexagonal-forming lipid, dioleoylphosphatidylethanolamine (DOPE). With up to 30 mole% lysolipid in DOPE, the mixture maintains the inverted hexagonal (H_{II}) phase in excess water, where increasing levels of lysolipid result in a systematic increase in the H_{II} lattice dimension. Analysis of the structural changes imposed by lysolipids show that, opposite to DOPE itself, which has an spontaneous radius of curvature (R_0) of -30 Å, PC lysolipids add high positive curvature, with $R_0 = +38$ to $+60$ Å, depending on chain length. LysoPEs, in contrast, add very small curvatures. When both polar group and hydrocarbon chains of the added lysolipid mismatch those of DOPE, the structural effects are qualitatively different from otherwise. Such mismatched lysolipids "reshape" the effective combination molecule into a longer and more cylindrical configuration compared to those lysolipids with either matching polar group or hydrocarbon chain.

INTRODUCTION

Evidence has been accumulating that suggests an important dynamic structural role for the various membrane lipids present in biological membranes. Not all membrane lipids are intrinsically bilayer forming. Some, for example phosphatidylethanolamines (PE), tend to form structures with negatively curved monolayers, and others, for example, lysophospholipids, the subject of the present investigation, tend to form structures with positive curvature. When incorporated into bilayers, such nonbilayer-forming lipids introduce packing stresses. Such stresses can, in turn, affect membrane integrity (Cullis and DeKruijff, 1979; Gruner, 1985; Zhelev, 1998), or influence the insertion, conformation, and activity of membrane-embedded proteins (Bezrukov et al., 1999; Dan and Safran, 1998; McCallum and Epand, 1995). It is understandable then, that the lipid composition of membranes is regulated and modulated by the cell.

Lysophospholipids usually are found only in small amounts in biological cell membranes (Reman et al., 1969). As intermediates in phospholipid metabolism and turnover, they are produced by phospholipase A_2 hydrolysis of diacylphospholipids (Brown et al., 1993; Baker et al., 1994), by oxidation of low-density lipoproteins (Quinn et al., 1988), or by lecithin:cholesterol acyltransferase action on plasma lipoproteins (Bhamidipati and Hamilton, 1995). Subsequently, they are rapidly reacylated (Robertson and Lands, 1964; Eibl et al., 1969; Van Golde et al., 1971) or metabolized (Pelech and Vance, 1989).

On their own, lysophospholipids are nonbilayer-forming lipids above the hydrocarbon melting temperature. With a relatively large hydrophilic head group in relation to the hydrocarbon tail, pure lysolipid molecules pack in highly curved structures. Micelles are formed at low lipid concentrations, whereas, at higher concentrations, a hexagonal phase is formed of lipid cylinders with hydrocarbon interiors in a water matrix (Rand et al., 1975).

In spite of their small proportion of the membrane lipid, lysophospholipids have been shown to play a role in a wide range of cellular processes that involve membrane–protein or membrane–membrane interactions. For example, lysophosphatidylcholine (PC) has been shown to potentiate diacylglycerol activation of protein kinase C (Sasaki et al., 1993) and the related T-lymphocyte activation (Asaoka et al., 1993b), and HL-60 cell differentiation (Asaoka et al., 1993a). The authors conclude that lysolipids, as products of phospholipase A_2 activation, may be directly involved in the signal transduction pathway through protein kinase C to induce long-term cellular responses. Other evidence of effects on membrane proteins include: regulation of guanylate and adenylate cyclase activities (Shier et al., 1976), inhibition of insulin receptor autophosphorylation and signaling (McCallum and Epand, 1995), and the increased expression of adhesion molecules on endothelial cells (Kume et al., 1992). Early reports of membrane structural properties affected by abnormal accumulations of lysophospholipid include induced cell fusion (Poole et al., 1970) and even lysis at high levels (Reman et al., 1969; Weltzien, 1979).

Attempts to understand the mechanisms of lysolipid's effects have led to numerous studies incorporating lysophospholipid in both model and biological membrane systems. Membrane electrical resistance is lowered (Van Zutphen and Van Deenen, 1967) and permeability is increased (Lee and Chan, 1977) by added lysophospholipid. Many more studies have examined effects on membrane fusion.

Received for publication 1 December 2000 and in final form 2 April 2001.

Address reprint requests to N. Fuller, Dept. of Biological Sciences, Brock University, St. Catharines, ON L2S 3A1, Canada. Tel.: 905-688-5550x4166; Fax: 905-688-1855; E-mail: nfuller@spartan.ac.brocku.ca.

© 2001 by the Biophysical Society

0006-3495/01/07/243/12 $2.00

Inhibition of fusion by low levels of membrane-incorporated lysophospholipid has been demonstrated in diverse experimental systems, including microsome–microsome fusion (Chernomordik et al., 1993), influenza hemaglutanin-mediated fusion (Chernomordik et al., 1997; Gunther-Ausborn et al., 1995) syncytia formation mediated by Sendai virus F protein (Yeagle et al., 1994), and baculovirus gp64 (Chernomordik et al., 1995c). Fusion of pure lipid bilayers in model systems is also inhibited by lysophospholipid (Chernomordik et al., 1995a; Yeagle et al., 1994). (For a review see Chernomordik et al., 1995b). Importantly, the effect of lysophospholipid depends on its location, whether in the outer or inner monolayer or symmetrically distributed. LysoPC and arachidonic acid differentially inhibit or promote fusion of vesicles to planar bilayers depending on their location (Chernomordik et al., 1995a) and lysoPC has no effect on virus–liposome fusion if symmetrically distributed in both monolayers of the liposome (Gunther-Ausborn et al., 1995). In a study of PEG- mediated fusion of lipid vesicles, lysoPC promoted fusion when symmetrically distributed, and inhibited fusion when present only in the outer monolayer (Wu et al., 1996). It has been suggested that the common effects of lysophospholipid on fusion in such diverse systems occurs at approximately the same concentration in the membranes, and may involve a common lipidic intermediate of the fusion event, the proposed "stalk" structure (Chernomordik et al., 1987; Leikin et al., 1987; Kozlov et al., 1989; Siegel, 1993; Chernomordik et al., 1995b). The stalk structure is a highly negatively curved lipidic connection between opposing monolayers that leads to hemifusion.

Lysolipids affect the gating kinetics of several membrane channels, including gramicidin channels in lipid bilayers (Lundbaek and Anderson, 1994). Lysolipids stabilize dimer formation between two peptide helices in apposing monolayers, forming an open channel, and lysoPC is more effective than lysoPE. These lysolipid effects are attributed to some property of the lipid that lowers the energy of bilayer deformation required for dimer formation.

The effects of lysophospholipids, i.e., disruption of intact membranes, lowering of electrical resistance, increasing permeability, inhibition of fusion, and effects on channel-gating kinetics are all consistent with models based on the dynamic shape of the molecule that packs with local positive curvature (Chernomordik et al., 1995b). When added to other lipids, lysolipids would tend to drive lipid assemblies into structures with more positive curvature. When confined to the bilayer phase, lysolipids would introduce membrane tensions or stresses that may influence the conformation and activity of membrane proteins.

We have measured the influence of various lysolipids on the spontaneous curvature of mixed lipid monolayers. "Spontaneous curvature " and "intrinsic curvature" are often used interchangeably. In this work, we are going to use spontaneous curvature and derive its value for individual lipid components. To do this, we have incorporated several different lysolipids into a nonbilayer structure, the negatively curved inverted hexagonal phase formed by DOPE in aqueous medium. We also measure any effect of lysolipids on the bending modulus of DOPE monolayers.

MATERIALS AND METHODS

Synthetic dioleoylphosphatidylethanolamine (DOPE) and six synthetic lysophospholipids were purchased from Avanti (Polar Lipids, Inc., Alabaster, Alabama), and used without further purification. The lysophospholipids differed from each other in chain length or headgroup, three of them being PC and three being PE. They were: laurylphosphatidylethanolamine (L-lysoPE), oleoylphosphatidylethanolamine (O-lysoPE), stearoylphosphatidylethanolamine (S-lysoPE), laurylphosphatidylcholine (L-lysoPC), oleoylphosphatidylcholine (O-lysoPC), and palmitoylphosphatidylcholine (P-lysoPC). *n*-Tetradecane was purchased from Sigma-Aldrick Canada Ltd. (Oakville, Ontario), and water used in the experiments was double-distilled.

Stocks of lipid mixtures were prepared first by combining DOPE and various amounts of one of the lysolipids in chloroform solution. The chloroform was then removed by rotary evaporation, followed by vacuum desiccation. Tetradecane was added to the dry lipid mixture to 16 wt% of the total, by weighing directly, and the mixture was allowed to equilibrate three days. Samples (each about 20 mg) from the lipid stocks were then hydrated to varying degrees by directly weighing in double-distilled water, or by adding excess amounts (2 ml) of polyethylene glycol solutions of known osmotic pressure. A further three days were allowed for equilibration of the water in the sample. Finally, equilibrated samples were mounted between mica windows with powdered teflon, as an x-ray calibration standard, and examined by x-ray diffraction.

X-ray diffraction patterns were used to characterize the structures and dimensions of the various phases formed. Patterns were collected on film using Guinier cameras mounted on a Rigaku rotating anode x-ray generator. The CuKα_1 line ($\lambda = 1.540$ Å) was used, isolated by a bent quartz crystal monochromator. For all experiments described, the temperature of the sample was controlled by thermoelectric elements to 22°C ± 0.2°C. Typically, hexagonal phases were observed, characterized by a series of x-ray spacings bearing ratios to the dimension of the first order, d_{hex}, of 1, $1/\sqrt{3}$, $1/\sqrt{4}$, $1/\sqrt{7}$, $1/\sqrt{9}$, $1/\sqrt{12}$, etc. At higher lysolipid contents, lamellar phases, characterized by x-ray spacing bearing the ratios 1, 1/2, 1/3, 1/4, etc, coexisted with the hexagonal phases. For the purpose of this study, we have restricted data analysis to the region of sample compositions producing single hexagonal phases. Lattice dimensions of the hexagonal structures could be measured to ± 0.1 Å on any one sample. Sample-to-sample variation, which includes all experimental errors, is approximately ±2%.

Structural analysis

H_{ii} phases are two-dimensional hexagonal lattices formed by the axes of indefinitely long and parallel regular prisms. Water cores, centered on the prism axes, are lined with the lipid polar groups, and the rest of the lattice is filled with the hydrocarbon chains.

For a hexagonal phase of known composition, the measured lattice can be divided into compartments, as shown in Fig. 1, each containing defined volume fractions of the lipid and water. This volume average division follows the method originally introduced by Luzzati (e.g., see Luzzati and Husson, 1962) and depends only on the assumption of their linear addition. Specific data for the lipid components used in these systems are given in Table 1.

In particular, we separate the water and lipid compartments in the hexagonal lattice by an idealized cylindrical interface of radius R_w that encloses a volume equal to the volume of water in the H_{ii} phase (Fig. 1).

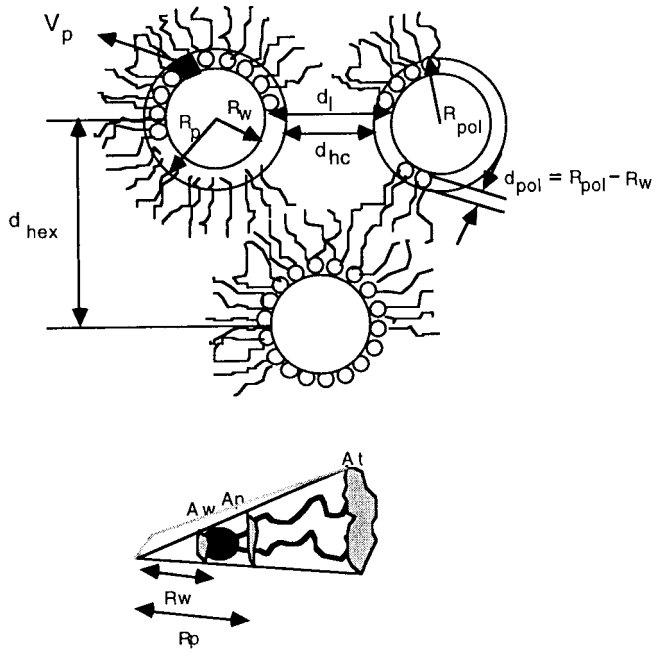

FIGURE 1 Schematic diagram of the structure of the hexagonal phase showing the dimensions determined as described in the text and used for the structural and energetic analysis.

We then use it for data analysis as if all the water is inside and all the lipid is outside of this cylinder. We refer to the surface of this cylinder as the Luzzati plane.

The radius of the water cylinder, R_w, is related to the first-order Bragg spacing in the hexagonal phase, d_{hex}, and to the volume fraction of water in the sample, ϕ_w, as follows:

$$R_W = d_{hex}\sqrt{\frac{2\phi_w}{\pi\sqrt{3}}}. \tag{1}$$

The area per lipid molecule at the Luzzati plane is given by

$$A_W = \frac{2\phi_W V_l}{(1-\phi_W)R_W}, \tag{2}$$

where V_l is the volume of a lipid molecule, and

$$\phi_W = \frac{V_{water}}{V_{water} + V_{PL} + V_{lysolipid} + V_{tetradecane}}. \tag{3}$$

For the calculation of molecular area in this study, we use the notion of an effective molecule, that is, one phospholipid + x lysolipids + y tetradecane molecules: x is the molar ratio of lysolipid to phospholipid, and y is the molar ratio of tetradecane to phospholipid in the samples. The effective molecular volume is

$$V_l = v_{PL} + x \cdot v_{lysolipid} + y \cdot v_{tetradecane}, \tag{4}$$

where v_{PL}, $v_{lysolipid}$, and $v_{tetradecane}$ are the molecular volumes of DOPE, lysolipid, and tetradecane. These equations determine structural parameters at the Luzzati plane, using d_{hex}, measured in the x-ray experiment, and ϕ_w, calculated from the weight fraction of water in the samples using the specific molecular volumes given in Table 1.

Elastic energy of the hexagonal phase

The H_{ii} phase is usually described in terms of curvature and molecular area on either of two cylindrical surfaces lying inside the lipid monolayer: 1) a neutral surface of bending where the bending and stretching (compression) deformations are energetically uncoupled (Kozlov and Winterhalter, 1991a,b); and 2) a pivotal plane where the molecular area remains constant (Rand et al., 1990). Here we analyze the experimental data using the pivotal plane, because its position can be found from the data with much higher accuracy (Leikin et al., 1996). Using the radius of curvature at the pivotal plane, R_p, the elastic free energy, F, of the hexagonal phase (normalized per effective molecule) can be approximated by the energy of bending (Helfrich, 1973; Kirk et al., 1984),

$$F = \frac{1}{2}K_{cp}A_p\left(\frac{1}{R_p} - \frac{1}{R_{0_p}}\right)^2, \tag{5}$$

where K_{cp} is the bending modulus, and A_p and R_{0p} are the molecular area and the spontaneous radius of curvature at the pivotal plane.

The goal of the measurement is to find the position of the pivotal plane, the spontaneous curvature, molecular area, and bending moduli for different phospholipid/lysophospholipid mixtures. These structural parameters and elastic moduli (Leikin et al., 1996) are determined as follows:

1. The molecular area, A, and radius of curvature, R, at any cylindrical dividing surface, separated by a volume V per lipid molecule from the Luzzati plane (Fig. 1) are related by

$$A^2 = A_W^2 + 2V\frac{A_W}{R_W} \tag{6}$$

TABLE 1 Molecular and density data of the molecules used in this study

	Molecular weight	Molecular weight hydrocarbon	Molecular weight polar group	Specific volume	Specific volume hydrocarbon
DOPE	744.0	475.0	269	1	1.17
L-lysoPC	439.5	128.5	311	0.88	1.17
O-lysoPC	521.7	210.7	311	0.926	1.17
P-lysoPC	495.6	184.6	311	0.911	1.17
L-lysoPE	397.5	128.4	269	0.845	1.17
O-lysoPE	479.6	210.6	269	0.901	1.17
S-lysoPE	481.6	212.6	269	0.902	1.17
Tetradecane	198.0	198.0		1.31	

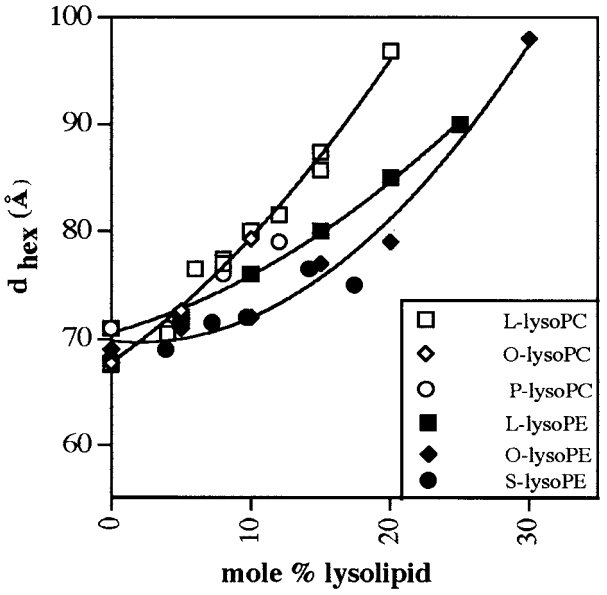

FIGURE 2 Plot of the equilibrium lattice spacing, d_{hex}, for lipid mixtures of increasing amounts of the indicated lysolipids in DOPE.

or

$$A = A_W \sqrt{1 + \frac{1 - \phi_W}{\phi_W} \frac{V}{V_1}},$$

$$R = R_W \sqrt{1 + \frac{1 - \phi_W}{\phi_W} \frac{V}{V_1}} \tag{7}$$

2. We verify whether the system has a well-defined pivotal plane by plotting A_w^2 versus A_w/R_w, from Eq. 6, in the form

$$A_w^2 = A_p^2 - 2V_p \frac{A_w}{R_w} \tag{8}$$

If the plot is a straight line, the system has a dividing surface of constant area, which is the pivotal plane. From the slope and the intercept of the plot, we determine the position of the pivotal plane, given by V_p, the volume separating this plane and the Luzzati plane, and the molecular area of an effective molecule at that plane, A_p.

3. From the value of V_p, we calculate the radii of curvature (R_p) at the pivotal plane by using Eq. 7. For each mixture under equilibrium conditions in excess water (determined from the phase diagrams), we determine the spontaneous radius of curvature at the pivotal plane (R_{0p}).

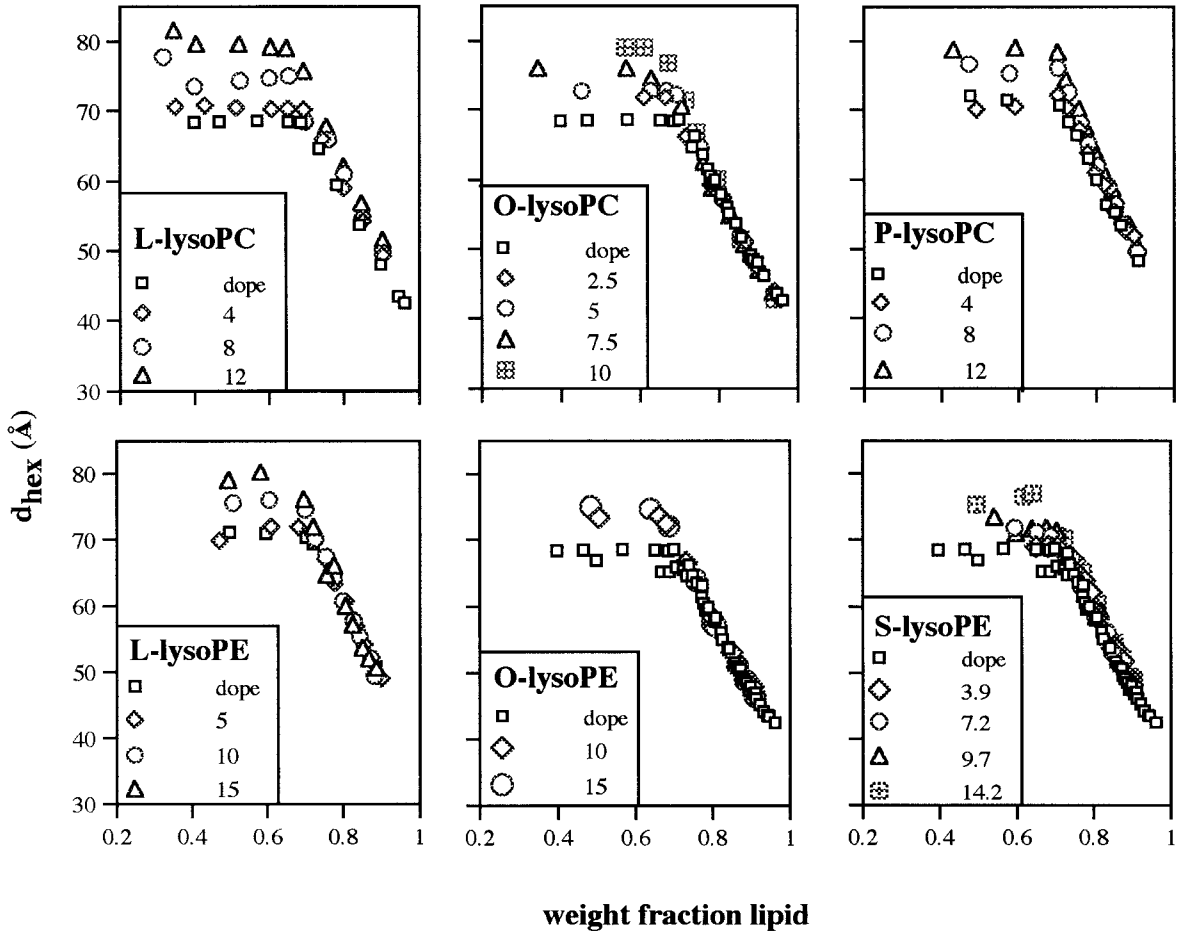

FIGURE 3 Lattice dimension, d_{hex}, as a function of water content for the hexagonal phases formed by DOPE containing the indicated mole% lysolipids.

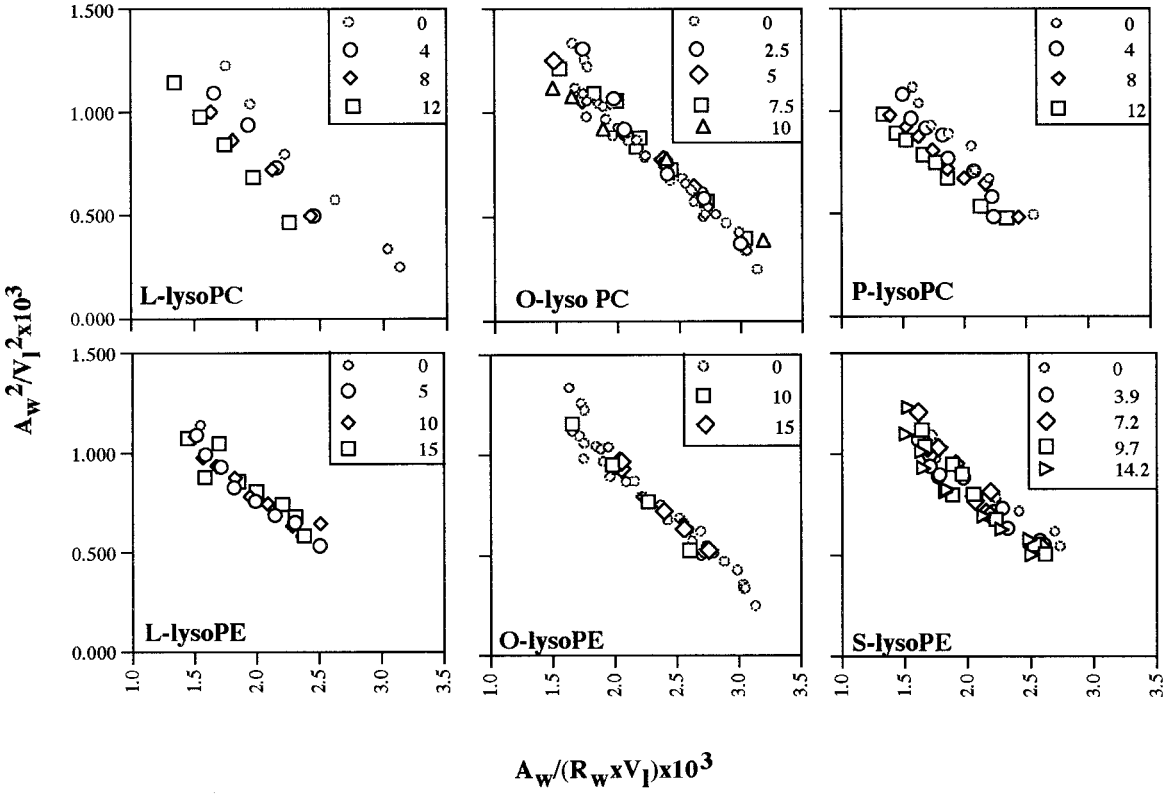

FIGURE 4 Diagnostic plots, in units of $Å^{-2}$ according to Eq. 8 of the text, for the lipid mixtures of Fig. 3. Linearity indicates a pivotal plane, the slope gives its position V_p/V_l, and the intercept, A_p/V_l, gives the area of an effective molecule at this plane.

4. The relation between the spontaneous radius of curvature, and the molar fraction of lysophospholipid, m_{lyso}, can give an apparent spontaneous radius of curvature for each of the components if

$$\frac{1}{R_{0p}} = (1 - m_{lyso})\frac{1}{R_{0p}^{DOPE}} + m_{lyso}\left(\frac{1}{R_{0_p}^{lyso}}\right) \quad (9)$$

is linear.

5. Finally, comparing the elastic energy given by Eq. 5 with the osmotic work done by the osmotic stress (π), we find the relationship,

$$\Pi R_p^2 = 2K_{cp}\left(\frac{1}{R_p} - \frac{1}{R_{0p}}\right). \quad (10)$$

A plot of (ΠR_p^2) versus $(1/R_p)$ gives, from the slope, the monolayer bending modulus (K_{cp}) (Gruner et al., 1986; Rand et al., 1990).

RESULTS

Throughout this work, we have kept tetradecane present at a constant 16 wt% of the total lipid fraction. The tetradecane is necessary to allow the formation of the larger dimension hexagonal phases, presumably allowing low monolayer curvature to be expressed by filling the interstitial spaces. (Rand et al., 1990; Chen and Rand, 1998). It is under these stress-free conditions and in excess water that we define and measure the spontaneous curvature of the mixed lipid monolayers from the lattice spacing d_{hex}.

To establish that lysolipid solubility in aqueous phases did not affect the composition of the x-ray samples, we noted the following. First, gravimetric samples containing lysolipids equilibrated with increasing amounts of excess water give identical spacings. Second, and more critically, the spacings of samples equilibrated with excess polymer solutions were unchanged when then re-equilibrated with more polymer solution after the first x-ray experiment. Therefore, we conclude that the partitioning of lysolipid from an aqueous phase into bulk lipid phases was so complete that our x-ray sample composition was as prepared.

Figure 2 shows the relation between mole percent lysolipid in DOPE and the equilibrium lattice spacing for the single hexagonal phase that is formed in excess water for six different lysolipids. In each case, the dimension of the hexagonal phase increases with increasing lysolipid content. This effect appears greater for the lysoPCs than for lysoPEs, especially evident at higher concentrations. At lysolipid concentrations higher than those plotted in Fig. 2, a lamellar phase coexists with the hexagonal phase in excess water, typical of mixtures of lipids with different spontaneous curvatures (Rand et al., 1990).

TABLE 2 Structural and elastic parameters for all mixtures of lipids at full hydration

Lipid (mole %lyso in DOPE)	Pivotal plane V_p/V_l	Wt. fraction Lipid, c	d_{hex} (Å)	R_w (Å)	R_{pol} (Å)	R_{op} (Å)	d_l (Å)	d_{hc} (Å)	$Area_w$ (Å^2)	$Area_p$ (Å^2)	$Area_t$ (Å^2)	Kc/kT
dope	0.32	0.713	68.5	21.9	27.0	29.6	35.4	25.0	54	73	107	12.2
4% L-lysoPC	0.32	0.710	70.6	22.7	27.8	30.6	36.2	25.8	54	73	107	12.0
8% L-lysoPC	0.32	0.693	75	24.8	29.9	32.8	37.0	26.7	55	73	106	12.4
12% L-lysoPC	0.32	0.673	79.7	27.2	32.3	35.4	37.5	27.4	56	73	105	11.8
dope	0.28	0.719	68.5	21.6	26.9	28.7	35.8	25.3	53	70	107	11.0
2.5% O-lysoPC	0.28	0.696	71.8	23.6	28.8	30.6	35.7	25.3	55	71	107	13.2
5.0% O-lysoPC	0.28	0.690	72.8	24.2	29.3	31.2	35.7	25.5	56	73	108	12.5
7.5% O-lysoPC	0.28	0.668	76.1	26.2	31.1	33.1	35.5	25.6	59	74	109	14.1
10.0% O-lysoPC	0.28	0.651	79.1	27.9	32.8	34.8	35.5	25.8	60	75	109	11.4
dope	0.31	0.706	71.0	22.9	28.2	30.6	36.1	25.6	53	71	105	
3.9% P-lysoPC	0.31	0.716	71.0	22.6	27.8	30.4	36.9	26.3	53	71	106	
7.9% P-lysoPC	0.31	0.700	76.0	24.8	30.1	32.9	38.1	27.5	53	70	104	
12.0% P-lysoPC	0.31	0.685	79.0	26.5	31.6	34.5	38.2	28.0	55	72.	105	
dope	0.26	0.724	71.0	22.2	27.7	29.1	37.5	26.5	50	66	102	9.2
5% L-lysoPE	0.26	0.717	72.0	22.9	28.2	29.7	37.4	26.7	52	68	104	9.4
10% L-lysoPE	0.26	0.689	76.0	25.3	30.4	32.1	37.1	26.9	55	70	106	9.7
15% L-lysoPE	0.26	0.663	80.0	27.8	32.7	34.4	36.8	27.0	58	72	107	9.7
dope	0.30	0.717	68.5	21.7	26.9	29.1	35.7	25.2	53	71	107	11.8
10% O-lysoPE	0.30	0.683	73.5	24.7	29.5	31.9	35.4	25.8	59	76	112	10.7
15% O-lysoPE	0.30	0.673	75.0	25.6	30.3	32.8	5.3	26.1	62	79	115	10.7
dope	0.26	0.729	68.5	21.2	26.6	28.1	36.6	25.8	51	68	105	10.0
3.9% S-lysoPE	0.26	0.726	69.0	21.5	26.8	28.3	36.6	26.1	52	69	107	9.6
7.2% S-lysoPE	0.26	0.709	71.5	23.0	28.1	29.8	36.5	26.3	55	71	108	9.4
9.7% S-lysoPE	0.26	0.706	72.0	23.3	28.3	30.0	36.5	26.5		72	110	9.6
14.2% S-lysoPE	0.26	0.680	76.0	25.7	30.5	32.4	36.3	26.8	59	75	112	8.5

Parameters are described in Figure 1 and methods.

When some of the lipid mixtures of Fig. 2 are dehydrated, a lamellar phase eventually appears because of the free energy balance between lamellar and hexagonal phases (Kozlov et al., 1994). Typically, ~12–15% lysolipid will be accommodated in the single hexagonal phase over the entire hydration range, with slightly more lysoPE accommodated than lysoPC. In this study, we report and analyze only the single hexagonal structures.

Gravimetric phase diagrams, covering the full hydration range, for various mixtures of the six lysolipids with DOPE, are shown in Fig. 3. The hexagonal phase dimension is shown here as a function of weight fraction of lipid in water. In each series, lysolipid was mixed in three or four different ratios with DOPE (from 0 to 12–15%). All samples gave single hexagonal phases at the lysolipid concentrations reported. The dimension of these phases can be seen to increase with water content until a maximum is reached. Further addition of water results in a separate water phase.

In less than excess water, for four of the six lysolipids examined, L-lysoPE, O-lysoPE, S-lysoPE, and O-lysoPC, the relation between lattice dimension and water content did not detectably depend on the lysolipid concentration in the sample. For L-lysoPC, and P-lysoPC, however, at any one water volume fraction, the lattice dimension increases systematically with increasing lysolipid content. This qualitative difference in behavior is more easily seen in the diagnostic plots of Fig. 4 and subsequent analysis.

The weight fraction of lipid at maximum hydration was determined from the intercept of the best fit curve below excess water, with the average maximum dimension in excess water. Equilibrium conditions and structural parameters can be calculated from the gravimetric phase diagrams of Fig. 3, according to the analysis described in the methods. These are shown in Table 2.

Pivotal plane

Figure 4 shows the diagnostic plots (Eq. 8) of $(A_w/V_l)^2$ versus $(A_w/V_l)R_w$ for all lysolipid/DOPE mixtures studied. The linearity of these relations shows that there exists a well-defined pivotal plane for all these lipid mixtures. Consistent with most lipid systems studied, there exists a position within the monolayer that does not change area even as the monolayer is bent on dehydration.

The position of the pivotal plane, given by the slope of the relations in Fig. 4, is defined as (V_p/V_l). For all mixtures, it lies close to the polar group hydrocarbon interface (V_{pol}/V_l). V_p/V_l ranges from 0.32–0.26 (Table 2). V_{pol}/V_l is 0.21. Therefore, the pivotal plane resides 1.8 + 0.7 CH_2 groups

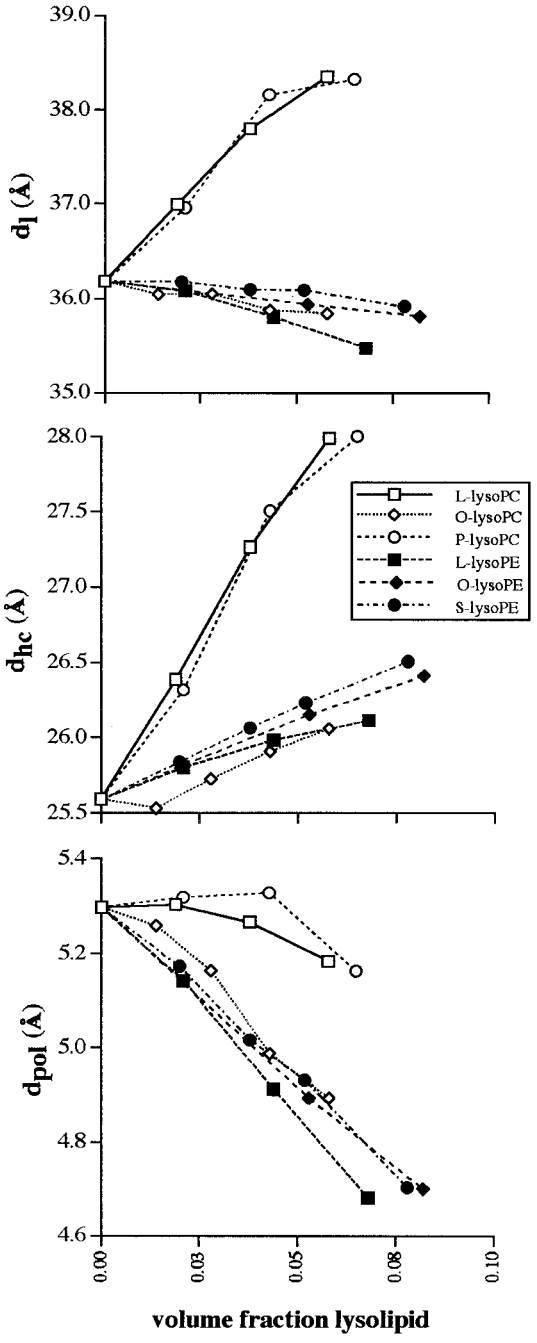

FIGURE 5 Plots of molecular dimensions d_l, d_{pol}, and d_{hc} (see Fig. 1) of DOPE–lysolipid mixtures as the lysolipid content increases. To emphasize trends, molecular dimensions were normalized using the appropriate DOPE control. Lysolipids that mismatch both polar and hydrocarbon chains of DOPE behave differently from those for which at least one part matches. Most of the change in d_l is in the hydrocarbon region.

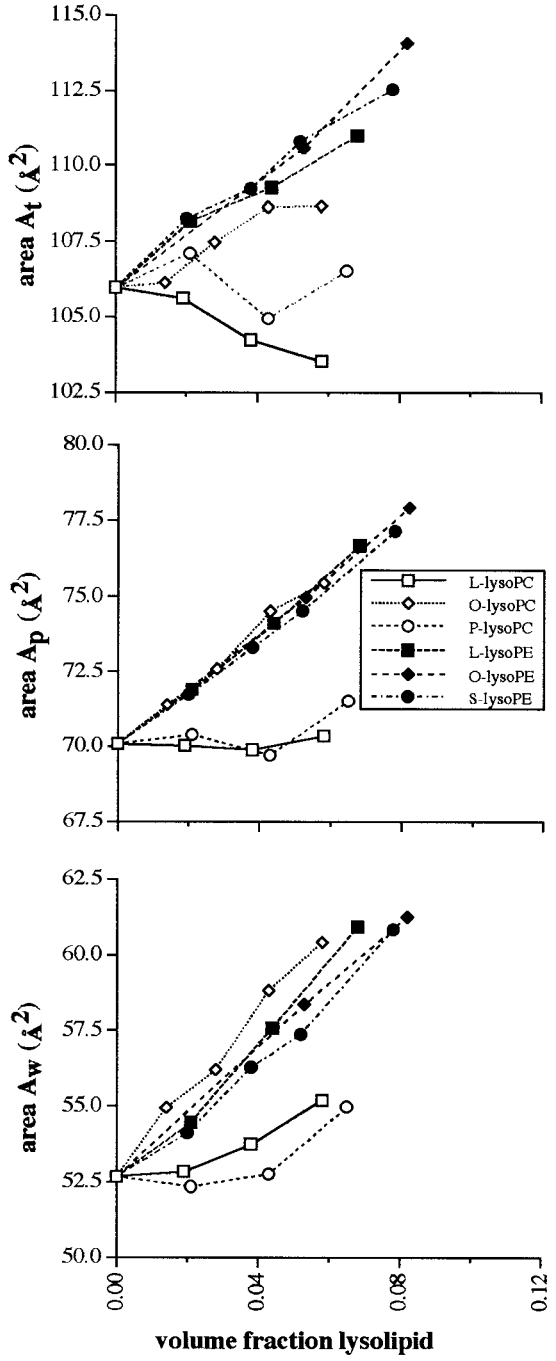

FIGURE 6 Molecular areas of the effective molecules of DOPE–lysolipid mixtures measured at the water–lipid interface, A_w, at the pivotal plane, A_p, and at the ends of the hydrocarbon chains, A_t, as the lysolipid content increases. To emphasize trends, molecular areas were normalized using the appropriate DOPE control. Lysolipids that mismatch both polar and hydrocarbon chains behave differently from those for which at least one part matches.

on the hydrocarbon side of the polar/hydrocarbon interface. In fact, for all other lipid systems examined to date, the pivotal plane lies close to the boundary between the hydrocarbon and polar group layers. Compared to positions away from the pivotal plane that can undergo large area changes, the pivotal plane itself behaves as if it is incompressible.

The intercepts of the relations of Fig. 4 give the molecular area per effective molecule at the pivotal plane (A_p/V_l). A_p/V_l does not change for each of the four lysolipids that show no effect of lysolipid content on lattice dimensions

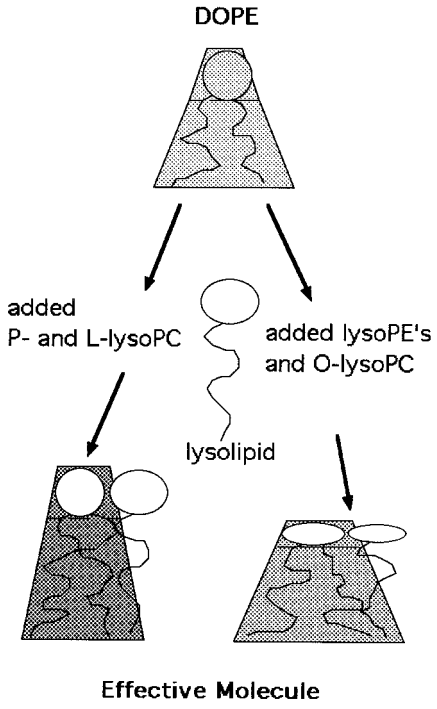

FIGURE 7 Schematic representation of the changes in molecular dimensions (Figs. 5 and 6) imposed on pure DOPE when doped with either L- or P-lysoPC, or with any of the other lysolipids. When both polar group and hydrocarbon chains mismatch those of DOPE, molecular areas change much less and the effective molecule is longer.

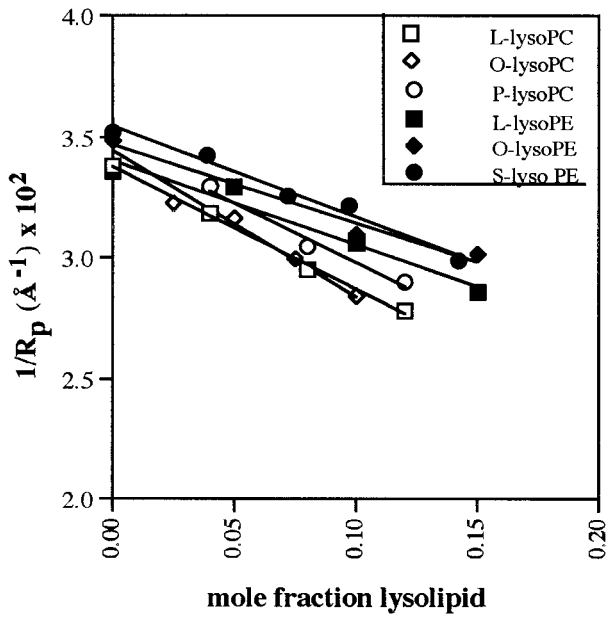

FIGURE 8 Plot of the DOPE monolayer curvature, $1/R_{op}$, as lysolipid content increases. The lysoPCs have a bigger effect than do the lysoPEs.

below excess water. This means that the area of the effective molecule at the pivotal plane, A_p, increases in proportion to the lysolipid concentration in the mixture, i.e., area increases with the size of the effective molecule V_l as one might expect. However, for L-lysoPC and P-lysoPC, (A_p/V_l) shifts with each lysolipid concentration. Remarkably, for these two mixtures, A_p is constant for all lysolipid concentrations even though the effective molecule is increasing in size.

The structural changes that occur (Table 2) appear to divide the added lysolipids into two qualitatively different groups. Figures 5 and 6 show that P- and L-lysoPCs have a different effect from the others. The molecular length, Fig. 5, of the effective molecule, d_l, increases as these lysolipids are added to DOPE while it remains relatively constant for the others. Most of that increase is in the hydrocarbon region, d_{hc}, while the polar group layer, d_{pol}, stays constant. In contrast, d_{pol} and d_{hc} change only slightly when the other lysolipids are added to DOPE.

Molecular areas (Fig. 6) show this different behavior. For P- and L-lysoPC, molecular area of the effective molecule changes much less with added lysolipid than for the others. Particularly striking is that the molecular areas away from the pivotal plane, A_w and A_t, are practically unchanged with added P- and L-lysoPC but increase at the water interface, making these effective molecules longer and more cylindrical. In contrast, the other effective molecules expand laterally with added lysolipid. We have attempted to convey this difference in behavior schematically in Fig. 7.

Spontaneous curvature

The radius of spontaneous curvature of the lipid mixtures, R_{0p}, is calculated from Eqs. 1 and 7 using the equilibrium volume fraction in excess water, the maximum lattice dimension for d_{hex}, and the value of V_p/V_l. Figure 8 shows how R_{0p} changes with lysolipid content for each of the lysolipids studied. As presumed from their effect on hexagonal dimension, lysolipids decrease monolayer curvatures. Generally, lysoPCs have a larger effect than lysoPEs, i.e., contribute more positive curvature, consistent with their larger polar group relative to hydrocarbon chain volume.

On the basis of the linear relation between the spontaneous curvature of the lipid mixtures and the mole fraction of lysolipid in those mixtures, the spontaneous curvatures of the individual lipids can be determined according to Eq. 9. These are shown in Table 3. They appear to be in two groups. First, L-, P-, and O-lysoPC have high positive curvatures. This would be expected from their larger ratio of polar group to hydrocarbon chain. Second, the lysoPEs have curvatures that are not detectably different from zero. The limitation in the amount of lysolipid that could be incorporated into the hexagonal phase before lamellar phases formed meant that this method could not reliably distinguish radii of curvatures greater than $\pm\sim$150 Å.

TABLE 3 Comparison of spontaneous radii of curvature and bending moduli for individual lipids as measured by the present methods

	R_0 (A)	K_c/kT	References
DOG (in DOPE)	−11.5		(Leikin et al. 1996)
DOG (in DOPC)	−10.1		(unpublished)
DCG (in DOPC)	−13.3		(unpublished)
DOPE	−28.5	11	(Leikin et al. 1996)
DOPE-tetradecane	−28.7	12	(Chen and Rand 1998)
CHOL (in DOPE)	−22.8		(Chen and Rand 1997)
CHOL (in DOPC)	−27.2 (32°C)		(Chen and Rand 1997)
DOPC	−87.3 (32°C)	9	(Chen and Rand 1997)
L-Lyso PE (in DOPE)	$R_o > 400$		
O-LysoPE (in DOPE)	$R_o > 400$		
S-Lyso PE (in DOPE)	$R_o > 400$		
L-Lyso PC (in DOPE)	+58		
O-Lyso PC (in DOPE)	+38		
P-Lyso PC (in DOPE)	+68		

Osmotic stress and bending modulus

The lattice dimensions, d_{hex}, of osmotically stressed hexagonal phases for five of the different mixtures were measured (data not shown). The water contents of these phases were determined from the known dependence of $ø_w$ versus d_{hex} in the gravimetric phase diagrams (Fig. 3). This allowed the calculation of other structural dimensions in these structures, in particular, R_p, the radius of curvature at the pivotal plane. According to Eq. (10), a plot of ΠR_p^2 versus $1/R_p$ gives, from the slope, the monolayer bending modulus, K_{cp}, at the pivotal plane. Figure 9 shows such plots for five lysolipids. The values of bending moduli and the change with lysolipid content are shown in Fig. 10 and Table 2. It is evident that lysolipids, at least to the amount that could be incorporated, had no detectable effect on the bending modulus of these monolayers.

DISCUSSION

The spontaneous curvature of individual molecules in monolayers and the resultant curvature stress within bilayer membranes is thought to affect both membrane protein activity and the energetics of topological changes in membranes such as those required by membrane fusion. Hence, we have been measuring spontaneous curvatures and effects on bending moduli for several lipids with the aim of being able to quantitate curvature stress. A compendium of results is shown in Table 3. LysoPCs at one extreme have curvatures opposite in sign to diacylglycerols on the other, both presumably contribute strongly to modulating membrane curvature stress.

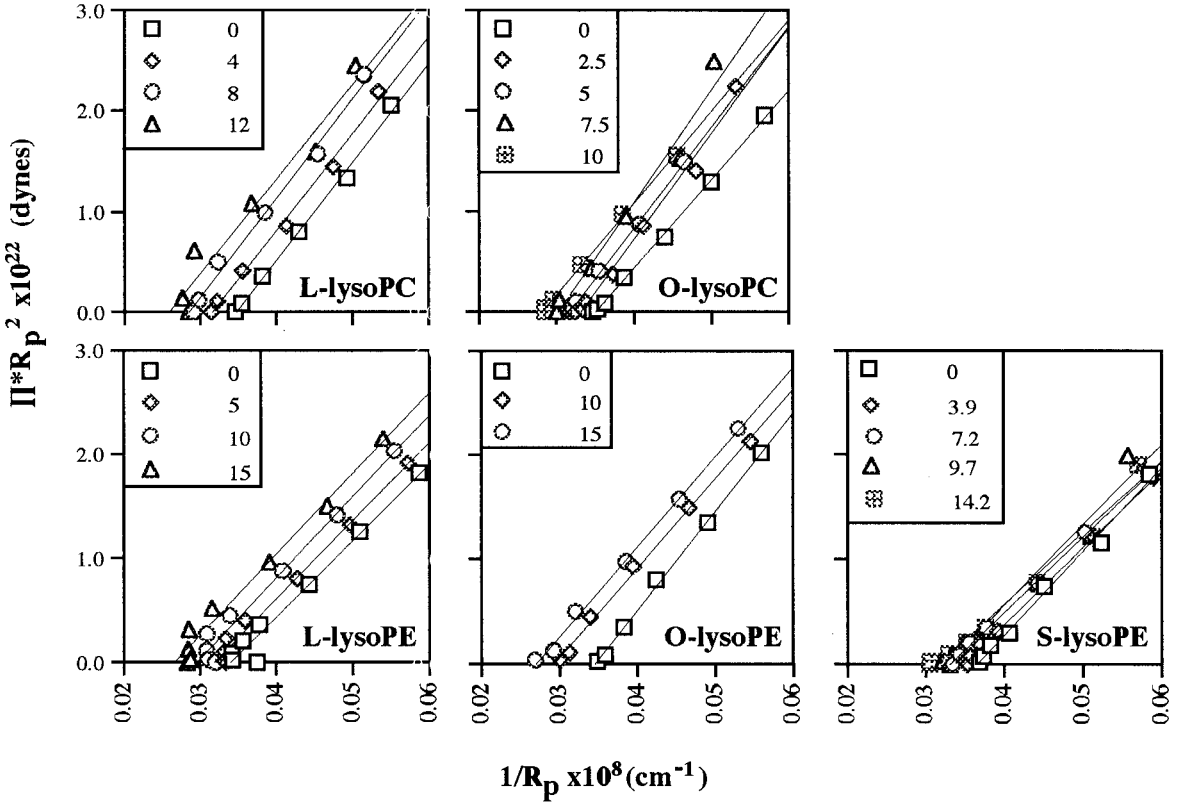

FIGURE 9 Plot relating the osmotic work required to dehydrate the hexagonal phase with its change in monolayer curvature $1/R_p$ (according to Eq. 10 of the text). The slope, which gives a measure of the bending modulus, shows no change with any species of lysolipid.

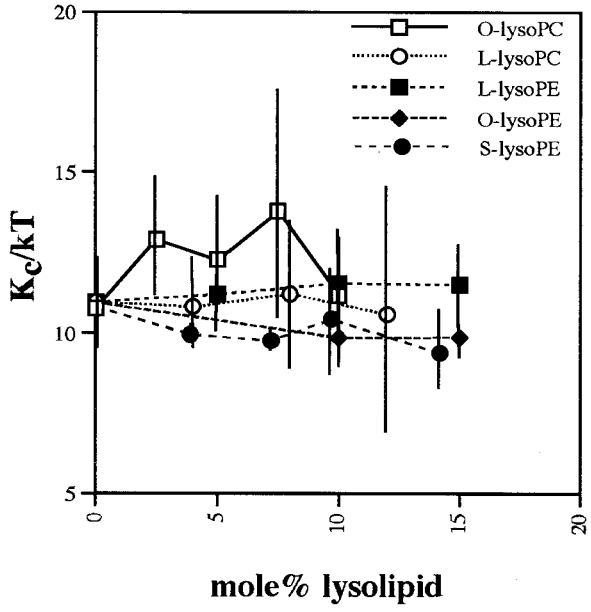

FIGURE 10 Plot of the bending moduli of DOPE doped with increasing amounts of lysolipids. Bending moduli were normalized using the appropriate DOPE control.

There are several steps in the stages of fusion that are affected by the spontaneous curvature of the participating lipids. Lysolipids in particular inhibit fusion when present on the proximal monolayers of approaching membranes, thought to result from inhibition of stalk formation by the nearest neighboring monolayers of approaching bilayers (Chernomordik et al., 1997). Lysolipids facilitate fusion when on the distal monolayers, thought to result from the formation and expansion of pores in the distal monolayers that form the hemifusion monolayer (Chernomordik et al., 1995a). The energetics of such lipid rearrangements have been estimated in models of membrane fusion (Kozlov et al., 1989) and the present results provide measurements of spontaneous curvatures and bending moduli to aid those estimates.

Figures 1 and 2 show that lysolipids strongly increase the lattice parameter of the hexagonal phase of DOPE up to the order of 100 Å. In the subsequent analysis, we show that this results from the addition of lipids with either extremely small or highly positive spontaneous curvature, opposite from that of the highly negative spontaneous curvature of the host lipid DOPE. This phenomenon is similar but opposite in direction to the effects of extreme negative curvature that diacylglycerols (Leikin et al., 1996), and cholesterol (Chen and Rand, 1997) have on phospholipid layers.

Analysis of the change in lattice dimensions as the monolayer of the hexagonal phase is bent by removal of water shows that there is a position near the interface between polar group and hydrocarbon chains that does not change in area. Such a pivotal plane has been found for all lipid mixtures in the present study, and in fact, for all lipid systems studied to date. Interestingly, the position of the pivotal plane appears very close to, but on the hydrocarbon side of the polar/hydrocarbon interface for all lipid systems studied. While changes in area at positions away from this pivotal plane can be large, the pivotal plane itself is a position within monolayers that is relatively incompressible. For incorporation into bilayers of inclusions like channels and proteins, the pivotal plane would appear to be the most difficult part of the monolayer to penetrate or expand.

We measure the curvature of the monolayer from the pivotal plane. The linear dependence of the curvature on lysolipid mole fraction gives the specific curvatures or curvature contribution of the individual lipids in the mixture. One limitation of the present system is the restricted amount of lysolipid that can be incorporated into the DOPE hexagonal phase before it becomes lamellar. That precludes a more accurate experimental estimate of the spontaneous curvature of the individual lipids. Nevertheless it is clear that lysolipid curvatures are either highly positive or very small. LysoPCs have a high positive curvature compared to lysoPEs as might be expected from the relative volume ratios of polar group to hydrocarbon chains of those two classes of molecules. LysoPCs, having higher positive curvatures, would be expected to modulate the local curvature stress in a membrane more effectively than lysoPEs. Interestingly, this structural result correlates with the potentiation of the activation of protein kinase C and related cellular responses by lysoPC and not by lysoPE (Asaoka et al., 1993a,b, Sasaki et al., 1993). Such modulation would be opposite that of diacylipids, as might be expected considering the relative ratio of polar and hydrocarbon molecular volume.

Another strong correlation connects the effects of lysoPCs and lysoPEs on the gating kinetics of membrane channels, particularly gramicidin. Lysolipids favor dimerization of gramicidin and the open state. LysoPCs, with higher positive curvature as measured in this study, yield longer open (dimer) lifetimes than lysoPEs (Lundbaek and Anderson, 1994) suggesting that curvature energy is important in reducing the energetics of bilayer deformation required for dimer formation.

The difference in behavior when both polar group and hydrocarbon chains of the lysolipid differ from the host lipid DOPE is remarkable. It suggests that, when there is a mismatch in both parts of the molecule, there results a different kind of interaction between DOPE and the lysolipid. The major difference is a relatively unchanging molecular area even away from the pivotal plane, suggesting a lower lateral compressibility coefficient stemming from free volume or packing defects at both the polar and hydrocarbon ends.

Our results cannot distinguish between homogenous and heterogeneous lateral distribution within the mono-

layer. An interesting possibility is that one might expect the shorter lysos to partition in the interaxial direction, and the longer to partition interstitially. In any case, the behavior of the two groups of lipid is different and might be pursued by techniques that measure the dynamics of lipid interactions.

We thank the Natural Sciences and Engineering Research Council of Canada for financial support.

REFERENCES

Asaoka, Y., K. Yoshida, Y. Sasaki, and Y. Nishizuka. 1993a. Potential role of phospholipase A_2 in HL-60 cell differentiation to macrophages induced by protein kinase C activation. *Proc. Natl. Acad. Sci. U.S.A.* 90:4917–4921.

Asaoka, Y., K. Yoshida, Y. Sasaki, Y. Nishizuka, M. Murakami, I. Kudo, and K. Inoue. 1993b. Possible role of mammalian secretory group II phospholipase A_2 in T-lymphocyte activation: implications in propagation of inflammatory reaction. *Proc. Natl. Acad. Sci. U.S.A.* 90:716–719.

Baker, B. L., B. C. Blaxall, D. A. Reese, G. R. Smith, and J. D. Bell. 1994. Quantification of the interaction between lysolecithin and phospholipase A_2. *Biochim. Biophys. Acta.* 1211:289–300.

Bezrukov, S. M., R. P. Rand, I. Vodyanoy, and V. A. Parsegian. 1999. Lipid packing stress and polypeptide aggregation: alamethicin channel probed by proton titration of lipid charge. *Faraday Discuss.* 111.

Bhamidipati, S. P., and J. A. Hamilton. 1995. Interactions of lyso 1-palmitoylphosphatidylcholine with phospholipids: a ^{13}C and ^{31}P NMR study. *Biochemistry.* 34:5666–5677.

Brown, S. D., B. L. Baker, and J. D. Bell. 1993. Quantification of the interaction of lysolecithin with phosphatidylcholine vesicles using bovine serum albumin: relevance to the activation of phospholipase A_2. *Biochim. Biophys. Acta.* 1168:13–22.

Chen, Z., and R. P. Rand. 1997. The influence of cholesterol on phospholipid membrane curvature and bending elasticity. *Biophys. J.* 73: 267–276.

Chen, Z., and R. P. Rand. 1998. Comparative study of the effects of several *n*-alkanes on phospholipid hexagonal phases. *Biophys. J.* 74:944–952.

Chernomordik, L., A. Chanturiya, J. Green, and J. Zimmerberg. 1995a. The hemifusion intermediate and its conversion to complete fusion: regulation by membrane composition. *Biophys. J.* 69:922–929.

Chernomordik, L., M. M. Kozlov, and J. Zimmerberg. 1995b. Lipids in biological membrane fusion. *J. Membrane Biol.* 146:1–14.

Chernomordik, L., E. Leikina, M. Cho, and J. Zimmerberg. 1995c. Control of baculovirus gp64-induced syncytium formation by membrane lipid composition. *J. Virol.* 69:3049–3058.

Chernomordik, L. V., E. Leikina, V. Frolov, P. Bronk, and J. Zimmerberg. 1997. An early stage of membrane fusion mediated by the low pH conformation of influenza hemagglutinin depends upon membrane lipids. *J. Cell Biol.* 136:81–93.

Chernomordik, L. V., G. B. Melikyan, and Y. A. Chizmadzhev. 1987. Biomembrane fusion: a new concept derived from model studies using two interacting planar lipid bilayers. *Biochim. Biophys. Acta.* 906: 309–352.

Chernomordik, L. V., S. S. Vogel, A. Sokoloff, H. O. Onaran, and E. Leikina. 1993. Lysolipids reversibly inhibit Ca^{2+}-, TP- and pH-dependent fusion of biological membranes. *FEBS Lett.* 318:71–76.

Cullis, P. R., and B. DeKruijff. 1979. Lipid polymorphism and the functional role of lipids in biological membranes. *Biochim. Biophys. Acta.* 559:399–420.

Dan, N., and S. A. Safran. 1998. Effect of lipid characteristics on the structure of transmembrane proteins. *Biophys. J.* 75:1410–1414.

Eibl, H., E. E. Hill, and W. E. M. Lands. 1969. The subcellular distribution of acyltransferases which catalyze the synthesis of phosphoglycerides. *Eur. J. Biochem.* 9:250–258.

Gruner, S. M. 1985. Intrinsic curvature hypothesis for biomembrane lipid composition: a role for nonbilayer lipids. *Proc. Natl. Acad. Sci. U.S.A.* 82:3665–3669.

Gruner, S. M., V. A. Parsegian, and R. P. Rand. 1986. Directly measured deformation energy of phospholipid H_{II} hexagonal phases. *Faraday Disc. Chem. Soc.* 81:29–37.

Gunther-Ausborn, S., A. Praetor, and T. Stegmann. 1995. Inhibition of influenza-induced membrane fusion by lysophosphatidylcholine. *J. Biol. Chem.* 270:29279–29285.

Helfrich, W. 1973. Elastic properties of lipid bilayers: theory and possible experiments. *Z. Naturforsch.* 28C:693–703.

Kirk, G. L., S. M. Gruner, and D. L. Stein. 1984. A thermodynamic model of the lamellar to inverse hexagonal phase transition of lipid membrane–water system. *Biochemistry.* 23:1093–1102.

Kozlov, M. M., S. Leikin, and R. P. Rand. 1994. Energetics of the reentrant hexagonal-lamellar-hexagonal transition in phospholipids. *Biophys. J.* 66:A299.

Kozlov, M. M., S. L. Leikin, L. V. Chernomordik, V. S. Markin, and Y. A. Chizmadzhev. 1989. Stalk mechanism of membrane fusion. *Eur. Biophys. J.* 17:121–129.

Kozlov, M. M., and M. Winterhalter. 1991a. Elastic moduli for strongly curved monolayers. Analysis of experimental results. *J. Physique.* 1:1085–1100.

Kozlov, M. M., and M. Winterhalter. 1991b. Elastic moduli for strongly curved monolayers. Position of the neutral surface. *J. Physique.* 1:1077–1084.

Kume, N., M. I. Cybulsky, and M. A. Gimbrone. 1992. Lysophosphatidlycholine, a component of artherogenic lipoproteins, induces mononuclear leucocyte adhesion molecules in cultured human and rabbit arterial endothelial cells. *J. Clin. Invest.* 90:1138–1144.

Lee, Y., and S. I. Chan. 1977. Effect of lysolecithin on the structure and permeability of lecithin bilayer vesicles. *Biochemistry.* 16:1303–1309.

Leikin, S., M. M. Kozlov, N. L. Fuller, and R. P. Rand. 1996. Measured effects of diacylglycerol on structural and elastic properties of phospholipid membrane. *Biophys. J.* 71:2623–2632.

Leikin, S. L., M. M. Kozlov, L. V. Chernomordik, V. S. Markin, and Y. A. Chizmadzhev. 1987. Membrane fusion: overcoming of the hydration barrier and local restructuring. *J. Theor. Biol.* 129:411–425.

Lundbaek, J. A., and O. S. Anderson. 1994. Lysophospholipids modulate channel function by altering the mechanical properties of lipid bilayers. *J. Gen. Physiol.* 104:645–673.

Luzzati, V., and F. Husson. 1962. The structure of the liquid-crystalline phases of lipid-water systems. *Journal of Cellular Biology* 12:207–219.

McCallum, C. D., and R. M. Epand. 1995. Insulin receptor autophosphorylation and signaling is altered by modulation of membrane physical properties. *Biochemistry.* 34:1815–1824.

Pelech, S. L., and D. E. Vance. 1989. Signal transduction via phosphatidylcholine cycles. *TIBS.* 14:28–30.

Poole, A. R., J. I. Howell, and J. A. Lucy. 1970. Lysolecithin and cell fusion. *Nature.* 227:810–813.

Quinn, M. T., S. Parthasarathy, and D. Steinberg. 1988. Lysophosphatidylcholine: a chemotactic factor for human monocytes and its potential role in atherogenesis. *Proc. Natl. Acad. Sci. U.S.A.* 85:2805–2809.

Rand, R. P., N. L. Fuller, S. M. Gruner, and V. A. Parsegian. 1990. Membrane curvature, lipid segregation, and structural transitions for phospholipids under dual-solvent stress. *Biochemistry.* 29:76–87.

Rand, R. P., W. A. Pangborn, A. D. Purdon, and D. O. Tinker. 1975. Lysolecithin and cholesterol interact stoichiometrically forming biomolecular lamellar structures in the presence of excess water, or lysolecithin or cholesterol. *Can. J. Biochem.* 53:189–195.

Reman, F. C., R. A. Demel, J. De Gier, L. L. M. Van Deenen, H. Eibl, and O. Westphal. 1969. Studies of the lysis of red cells and bimolecular lipid leaflets by synthetic lysolecithins, lecithins and structural analogs. *Chem. Phys. Lipids.* 3:221–233.

Robertson, A. F., and W. E. M. Lands. 1964. Metabolism of phospholipids in normal and spherocytic human erythrocytes. *J. Lipid Res.* 5:88–93.

Sasaki, Y., Y. Asaoka, and Y. Nishizuka. 1993. Potentiation of diacylglycerol-induced activation of protein kinase C by lysophospholipids. *FEBS Lett.* 320:47–51.

Shier, W. T., J. H. Baldwin, M. Nilsen-Hamilton, R. T. Hamilton, and N. M. Thanassi. 1976. Regulation of guanylate and adenylate cyclase activities by lysolecithin. *Proc. Natl. Acad. Sci. U.S.A.* 73:1586–1590.

Siegel, D. P. 1993. Energetics of intermediates in membrane fusion: comparison of stalk and inverted micellar intermediate mechanisms. *Biophys. J.* 65:2124–2140.

Van Golde, L. M. G., B. Fleischer, and S. Fleischer. 1971. Some studies on the metabolism of phospholipids in golgi complex from bovine and rat liver in comparison to other subcellular fractions. *Biochim. Biophys. Acta.* 249:318–330.

Van Zutphen, H., and L. L. M. Van Deenan. 1967. The effect of lysolecithin on the electrical resistance of lecithin bilayer membranes. *Chem. Phys. Lipids.* 1:389–391.

Weltzien, H. U. 1979. Cytolytic and membrane-perturbing properties of lysophosphatidylcholine. *Biochim. Biophys. Acta.* 559:259–287.

Wu, H., L. Zheng, and B. R. Lentz. 1996. A slight asymmetry in the transbilayer distribution of lysophosphatidylcholine alters the surface properties and poly(ethylene glycol)-mediated fusion of dipalmitoylphosphatidylcholine large unilamellar vesicles. *Biochemistry.* 35: 12602–12611.

Yeagle, P. L., F. T. Smith, J. E. Young, and T. D. Flanagan. 1994. Inhibition of membrane fusion by lysophosphatidylcholine. *Biochemistry.* 33:1820–1827.

Zhelev, D. V. 1998. Material property characteristics for lipid bilayers containing lysolipid. *Biophys. J.* 75:321–330.